Journal of Supramolecular Structure 9:299–326 (1978)
Transmembrane Signaling 283–310

Spin Label Studies on Rat Liver and Heart Plasma Membranes: Effects of Temperature, Calcium, and Lanthanum on Membrane Fluidity

Larry M. Gordon, Richard D. Sauerheber, and Judy A. Esgate

Lutcher Brown Center for Diabetes and Endocrinology, Scripps Clinic and Research Foundation, La Jolla, California 92037 and California Metabolic Research Foundation, La Jolla, California 92038

The structures of rat liver and heart plasma membranes were studied with the 5-nitroxide stearic acid spin probe, I(12,3). The polarity-corrected order parameters (S) of liver and heart plasma membranes were independent of probe concentration only if experimentally determined low I(12,3)/lipid ratios were employed. At higher probe/lipid ratios, the order parameters of both membrane systems decreased with increasing probe concentration, and these effects were attributed to enhanced nitroxide radical interactions. Examination of the temperature dependence of approximate and polarity-corrected order parameters indicated that lipid phase separations occur in liver (between 19° and 28° C) and heart (between 21° and 32° C) plasma membranes. The possibility that a wide variety of membrane-associated functions may be influenced by these thermotropic phase separations is considered.

Addition of 3.9 mM $CaCl_2$ to I(12,3)-labeled liver plasma membrane decreased the fluidity as indicated by a 5% increase in S at 37° C. Similarly, titrating I(12,3)-labeled heart plasma membranes with either $CaCl_2$ or $LaCl_3$ decreased the lipid fluidity at 37° C, although the magnitude of the La^{3+} effect was larger and occurred at lower concentrations than that induced by Ca^{2+}; addition of 0.2 mM La^{3+} or 3.2 mM Ca^{2+} increased S by approximately 7% and 5%, respectively. The above cation effects reflected only alterations in the membrane fluidity and were not due to changes in probe–probe interactions. Ca^{2+} and La^{3+} at these concentrations decrease the activities of such plasma membrane enzymes as Na^+, K^+-ATPase and adenylyl cyclase, and it is suggested that the inhibition of these enzymes may be due in part to cation-mediated decreases in the lipid fluidity.

Key words: lanthanum, calcium, lipid phase separation, lipid clusters, spin label method, membrane fluidity, temperature

Received February 26, 1978; accepted July 26, 1978.

0091-7419/78/0903-0299$04.70

Biological membranes have been proposed to exist as a fluid mosaic [1]. According to this model, a lipid bilayer forms the matrix with integral proteins embedded in the plane of the membrane. An essential feature of this model is that the lipids of functional cell membranes at physiological temperatures are in a fluid rather than a solid or gel state. Thus, the protein and lipid components would be expected to undergo rotational and translational motions and should also, in general, be randomly distributed. Numerous physical–biochemical investigations on biomembranes have provided experimental support for the fluid mosaic model. For example, differential scanning calorimetry studies indicate that the lipid gel to liquid-crystalline phase transitions in such cholesterol-poor membranes as sarcoplasmic reticulum [2] and rat liver microsomes and mitochondria [3] occur at temperatures much lower than physiological. Several ESR and fluorescence studies have indicated that appropriately labeled lipids are able to undergo rapid translational diffusion in the plane of either model or biological membranes [4]. Furthermore, various integral proteins diffuse in the membrane at rates that are determined, at least in part, by the lipid fluidity. It should be emphasized that Singer and Nicolson did not exclude the possibility that short-range, nonrandom interactions may occur either between lipids and integral proteins or between certain integral proteins (eg, interactions between components of the electron-transport chain) [1].

However, recent studies suggest that the fluid mosaic model may be over-simplified in that lipid domains of differing structure and/or fluidity may coexist in either model or biological membranes. The formation of "quasi-crystalline" clusters in dioleoyl lecithin (DOL) and sarcoplasmic reticulum at temperatures above their respective "bulk" lipid-melting temperatures at $-22^{\circ}C$ and $10^{\circ}C$ was proposed by Lee et al [5] to explain the partitioning of the spin-label 2,2,6,6-tetramethylpiperidine-1-oxyl (Tempo) between the lipid and aqueous phases. Lee and co-workers viewed these clusters as being short-lived and as having both higher molecular densities and lower fluidities than the freely dispersed molecules. It is also possible that the cholesterol present in biological membranes preferentially associates with specific lipids, thereby creating domains of differing fluidity [6]. Phillips and Finer [7] proposed on the basis of their NMR experiments that mixed lecithin-cholesterol bilayers, which have less than equi-molar concentrations of cholesterol, will contain both short-lived (ie, lifetimes $\sim$ 30 msec) clusters of lecithin:cholesterol at a 1:1 ratio and clusters of free lecithin molecules. Distinct lipid phases might also be formed in biomembranes by the binding of divalent cations such as Ca^{2+}, as has been observed in a variety of artificial membranes [8–11]. Also, evidence has been obtained which suggests that immiscible fluid domains may occur in either binary mixtures of dipalmitoylphosphatidylethanolamine and dielaidoylphosphatidylcholine [12] or Bacillus stearothermophilus membranes [13]. Lee [6] and Jain and White [4] have reviewed numerous membrane functions that might be regulated by lipid domains or clusters. Nevertheless, the existence of physically distinct lipid domains might easily be overloooked in a given experiment, if such structures were short-lived or associated on the basis of weak interactions.

The interpretation of any results obtained using membranes labeled with spin probes may be complicated by the presence of distinct lipid domains or clusters. The spin-label method has been widely employed to study the dynamic properties of model and biological membranes. Depending on the design of the ESR experiment, it is possible to extract information on various motions of the membrane-incorporated spin probe [14]. The I(m,n)

label has been found to be particularly useful.

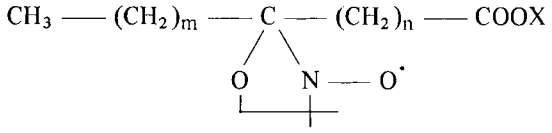

I(m,n)

A polarity-corrected order parameter (S) [15] that measures the flexibility of the lipid chains may be calculated from the outer and inner hyperfine splittings (ie, $2T_{||}$ and $2T_{\perp}$) of I(m,n)-labeled membrane spectra. The measurement of the S of a labeled membrane system therefore permits a direct determination of the "fluidity" of the bilayer. However, recent studies of several binary phase, model lipid systems indicate that I(m,n) probes preferentially partition into the more fluid phase [16–18]. If the I(m,n) label is similarly excluded from domains consisting of lipids in the gel or cluster state, the calculated S might indicate an unusually fluid environment that is not representative of the entire membrane.

An additional difficulty in performing membrane ESR studies is that the presence of nitroxide radical interactions may interfere with the measurement of the lipid fluidity. The selective solubility of I(m,n) in the membrane could result in high effective probe concentrations in the local lipid domains, even if a low probe/*total lipid* ratio is used. We have previously observed that "intrinsic" properties of I(12,3)-labeled rat liver and heart plasma membranes are assessed only if an experimentally determined low probe/lipid ratio is employed [19]. Here, "intrinsic" properties are defined as those which are measured when probe–probe interactions are negligible and do not refer to membrane behavior in the absence of a perturbing spin label.

The structures of rat liver and heart plasma membranes were further studied with the I(12,3) spin label as reported in the present paper. The temperature dependence of various spectral parameters was examined for membranes labeled with a wide range of I(12,3) probe concentrations. Thermotropic lipid phase separations that perturb the motion of the probe and may mediate a segregation of the probe at lower temperatures were observed in both membrane systems. We also report that titrating liver or heart plasma membranes with Ca^{2+} decreases the respective lipid fluidities at 37°C; La^{3+} additions to labeled heart plasma membranes similarly lower the lipid fluidity.

METHODS AND MATERIALS

Materials

The N-oxyl-4′, 4′- dimethyloxazolidine derivative of 5-ketostearic acid, I(12,3), was obtained from Syva Co, Palo Alto, California. Male Sprague-Dawley rats were purchased from Holtzman Co, Madison, Wisconsin. Sucrose was from Calbiochem, La Jolla, California, and all other chemicals were from Sigma Chemical Co, St. Louis, Missouri. Liquid nitrogen storage tubes were obtained from Microbiological Associates, Los Angeles, California, and 50 μl micropipettes were from Drummond Scientific Co.

Preparation and Characterization of Rat Liver and Heart Plasma Membranes

Liver plasma membrane was prepared essentially according to Evans [20] by centrifuging crude nuclear fractions from liver homogenates in a reorienting sucrose density gradient zonal rotor. The degree of membrane purification was determined by: (1) assigning the activities of both the plasma membrane enzymes 5′-nucleotidase and Na^+,K^+-ATPase and also the mitochondrial enzyme monoamine oxidase; and (2) phase-contrast microscopy. Liver membrane samples were suspended in 8% sucrose, 5 mM Tris-HCl (pH 7.6) and stored in liquid nitrogen storage tubes at −70°C [21].

Cardiac sarcolemma was purified according to the sucrose density gradient centrifugation procedure of Kidwai et al [22] with several modifications [23]. The plasma membrane fraction, which collected at the interface of the loading medium (8% sucrose) and the linear sucrose gradient (30–68.4% w/v), exhibited highly enriched specific activities of 5′-nucleotidase (from 5- to 10-fold) and minimal activity from the mitochondrial marker enzyme cytochrome c oxidase. Electronmicroscopic analysis of the putative plasma membranes indicated a large number of double membrane vesicles with diameters ranging from 700 Å to 4,000 Å. These results suggest that the purity of our plasma membrane fraction is similar to that obtained by Kidwai et al, [22]. Details of the preparation of the heart plasma membranes will be published elsewhere [23]. The sarcolemma fraction was suspended in 8% sucrose, 100 mM Tris-HCl (pH 7.5); only freshly prepared cardiac membranes were employed in this study.

Spin Labeling of Liver Plasma Membranes

The I(12,3) probe was dissolved in ethanol (10^{-3}M), and various aliquots were dried with a stream of dry N_2 gas in liquid nitrogen storage tubes. 120 μl samples of liver plasma membrane (3.3 mg membrane protein), stored until use at −70°C, were then added to the probe and gently vortexed for several min at room temperature. The spin label/membrane ratio employed was 0.7 to 4.1 μg I(12,3)/mg of liver plasma membrane protein. Spectra were recorded in a 150 μl capacity aqueous cell with a Varian E-3 ESR spectrometer equipped with a variable temperature accessory (see below). The temperature was calibrated from 15° to 40°C using a thermocouple placed in the resonant cavity. The microwave power was kept at 40 mW, which did not heat the sample or saturate the ESR signal [19].

Spin Labeling of Heart Plasma Membranes

80 μl samples containing approximately 160 μg cardiac sarcolemmal protein, stored until use at 4°C, were added to the I(12,3) probe following the procedure described above. The spin label/membrane ratios were varied from 14 to 235 μg I(12,3)/mg sarcolemmal protein. Spectra were recorded with a Varian E-104A Century Series ESR spectrometer equipped with a variable temperature accessory (see below). Micropipettes containing the labeled membrane samples were placed in a special holder (designed by R. D. Kornberg [24]), which was mounted in the temperature accessory. A thermocouple readout meter (Omega Engineering, Stamford, Connecticut) with 0.01-mm diameter wires leading to the center of the cavity indicated the sample temperature throughout each experiment. The microwave power was kept at 10 mW, which neither heated the sample nor saturated the ESR signal [19].

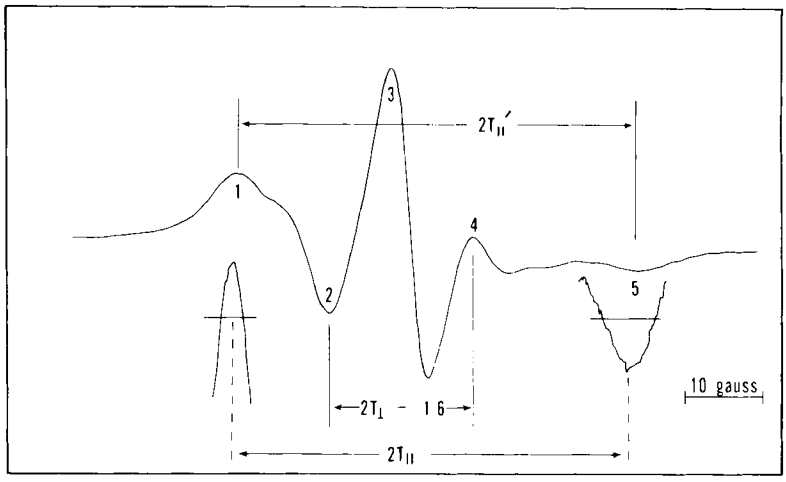

Fig 1. ESR spectrum of rat heart plasma membrane (37°C) labeled with 25 μg I(12,3)/mg membrane protein. The "unexpanded" spectrum was recorded with a 100 gauss field sweep, 5×10^4 receiver gain, 4 min scan time, and 1 sec time constant. $T_{||}'$ and $T_{\perp}$ were measured as shown: $2T_{\perp}$ was corrected by the addition of 1.6 gauss [15]. The outer wings 1 and 5 were "magnified" by recording with a 100 gauss field sweep, 5×10^5 receiver gain, 16 min scan time, and 1 sec time constant. $2T_{||}$ was measured from the magnified wings as indicated in Materials and Methods. Peak 4 is referred to in the text as the high-field peak of the inner hyperfine doublet.

Spectral Measurements

The hyperfine splittings of labeled liver and heart membranes were determined with several recording techniques. An "unexpanded" spectrum of I(12,3)-labeled rat cardiac sarcolemma is shown in Figure 1, which was recorded on a Varian E-104A ESR spectrometer with a 100 gauss field sweep, 5×10^4 receiver gain, four min scan time, and 1 sec time constant. Similar unexpanded spectra were previously obtained from liver plasma membranes labeled with a low I(12,3) probe concentration [19]. Only the relative positions of the maxima and minima were used to determine $T_{||}'$ and $T_{\perp}$. Errors associated with positioning the peaks in the unexpanded spectrum usually preclude splitting determinations more precise than 0.1 to 0.2 gauss.

Ehrenberg and co-workers [25] measured the outer splittings of I(12,3)-labeled Bacillus subtilis membranes by separately recording the outer peaks with a high gain and slow scan time. Following this procedure with labeled heart membranes, we recorded the outer wings (peaks 1 and 5 in Figure 1) on a Varian E-104A ESR spectrometer with a 5×10^5 receiver gain, 16 min scan time, and 1 sec time constant. The position of each peak was determined from the intersection of a horizontal line with the curved portion of the trace; the mid-distance between the intersection points was defined as the peak position. The precision of the $T_{||}$ value obtained using the "unexpanded with magnified wings" procedure was somewhat less than that which Ehrström et al. [25] found with labeled bacterial membranes (ie, the standard deviations were 0.08 and 0.05 gauss, respectively). The unexpanded with magnified wings procedure was used to record all heart plasma membrane ESR data presented in this paper.

It should be noted that the low and high field magnified peaks in Figure 1 were shifted downfield by approximately 1 gauss from the corresponding positions of the unmagnified peaks. This small displacement in the magnetic field plot was the result of changing the sweep time from 4 to 16 min and was not due to the increased gain setting. Control spectra of I(12,3)-labeled heart membranes were recorded as in Figure 1, except that the filter time constant was varied. The discrepancies in peak positions were minimized as the time constant was decreased from 4 to 0.128 sec. These results suggest that the use of a 1 sec time constant in Figure 1 introduced time-constant averaging into the unexpanded spectra. However, the slight distortion present in the unexpanded spectra does not apparently affect the accuracy of the hyperfine splittings reported here, since (1) $2T_{||}$ and $2T_{||}'$ of Figure 1 agreed to within experimental error, due to the shift of both magnified peaks in the same direction, and (2) the $2T_{||}$, $2T_{||}'$, and $2T_{\perp}$ values of labeled heart membranes were independent of the time constant for the range 0.128 to 2 sec.

Spectra of labeled liver and heart membranes were also recorded with the "expansion-superposition" method [19, 26]. Here, a spectrum such as Figure 1 was "expanded" by (1) recording pairs of adjoining numbered peaks with a field sweep smaller than 100 gauss and (2) superposing the common peaks. All order parameters of I(12,3)-labeled rat liver plasma membrane reported in this paper were calculated from expanded spectra, recorded with a Varian E-3 ESR spectrometer as described previously [19]. The expansion technique, modified for use on a Varian E-104A ESR spectrometer, was also used to record the spectra of I(12,3)-labeled rat heart plasma membrane (data not shown) [23]. With either the E-3 or E-104A ESR spectrometer, the expansion technique permits more precise measurement of the hyperfine splittings than may be obtained from conventionally recorded spectra.

Evaluation of the Flexibility of the Membrane-Incorporated I(12,3) Probe

In a previous paper [26] we derived the following order parameter expressions to assess the fluidity of fatty acid spin-labeled membranes in those cases in which either the inner or outer hyperfine extrema are not well defined.

$$S(T_{||}) = \tfrac{1}{2}\left[\frac{3(T_{||} - T_{xx})}{(T_{zz} - T_{xx})} - 1\right] \tag{1}$$

and

$$S(T_{\perp}) = \tfrac{1}{2}\left[\frac{3[(T_{zz} + T_{xx}) - 2T_{\perp}]}{(T_{zz} - T_{xx})} - 1\right] \tag{2}$$

Here, T_{xx} and T_{zz} are the hyperfine splitting elements of the static interaction tensor ($\underline{T}$) parallel to the static Hamiltonian ($\underline{H}$) principal nuclear hyperfine axes x and z, respectively. The x axis is parallel to the N–O bond direction, and the z axis is parallel to the nitrogen $2p\pi$ orbital. The elements of $\underline{T}$ used in this study were previously determined by incorporating nitroxide derivatives into host crystals as substitutional impurities: $(T_{xx}, T_{zz}) = (6.1, 32.4)$ gauss [27]. The elements of the effective hyperfine tensor ($\underline{T}'$), $T_{||}$ and $T_{\perp}$, were measured from the paramagnetic spectra of I(12,3)-labeled liver or heart membranes as shown in Figure 1. It should be noted that $S(T_{||})$ has been previously derived for nitroxide labels undergoing rapid anisotropic motion in the membrane [28, 29].

The expressions for $S(T_{||})$ and $S(T_{\perp})$ may be used to evaluate the average motion of the spin label in the membrane if (1) the probe undergoes rapid rotational and segmental motion so that the effective Hamiltonian ($\underline{H}'$) is axially symmetrical; (2) the polarity of the environment of the probe is identical to the corresponding polarity of the host crystal; and (3) "magnetically" dilute label concentrations are employed, since higher order terms representing probe–probe interactions are not included in $\underline{H}'$. For example, we previously reported that $T_{\perp}$ (but not $T_{||}$) broadened with increasing I(12,3) concentration in liver and heart plasma membranes at high probe/lipid ratios [19]. If any of the above conditions are not satisfied, $S(T_{||})$ and $S(T_{\perp})$ will not, in general, be equal, and the respective order parameters will serve only as approximate indicators of membrane fluidity.

However, an order parameter that corrects for polarity differences between the membrane and reference crystal may be calculated if both hyperfine splittings are available. Appropriate corrections to $S(T_{||})$ and $S(T_{\perp})$ may be applied by noting that the isotropic hyperfine coupling constant (a_N) is sensitive to the polarity of the environment of the nitroxide radical. Here, a_N' and a_N are the isotropic hyperfine coupling constants for the probe in the membrane and crystal state, respectively:

$$a_N = 1/3 \cdot (T_{zz} + 2T_{xx}) \tag{3}$$

$$a_N' = 1/3 \cdot (T_{||} + 2T_{\perp}) \tag{4}$$

Let us assume that changes in the polarity of the environment affect T_{xx} and T_{zz} in the same way. Equations (1) and (2) may then be corrected by dividing the elements of $\underline{T}$ (and $\underline{T}'$) by their respective hyperfine coupling constants a_N (and a_N'). Performing this operation on either $S(T_{||})$ or $S(T_{\perp})$ yields the polarity-corrected order parameter (S) initially derived by Hubbell and McConnell [15]:

$$S = \frac{T_{||} - T_{\perp}}{T_{zz} - T_{xx}} \quad \frac{a_N}{a_N'} \tag{5}$$

The order parameter S is therefore sensitive to the membrane fluidity (or, more accurately, the flexibility of the membrane-incorporated probe), if experimentally determined low I(m,n) concentrations are employed. S, $S(T_{||})$ and $S(T_{\perp})$ may assume values between 0 and 1; these extreme order parameters indicate that the probe samples fluid and immobilized environments, respectively.

RESULTS

ESR Spectra and Order Parameters of I(12,3)-Labeled Rat Heart and Liver Plasma Membranes

The effects of a wide range of I(12,3) probe concentrations on the ESR spectra of rat cardiac sarcolemma at 37°C were investigated. Figure 2A shows that the spectrum of sarcolemma labeled with an experimentally determined "low" probe concentration may be interpreted in terms of a membrane-incorporated I(12,3) label undergoing rapid, anisotropic motion about its long molecular axis. A number of spectral alterations occurred as the probe concentration increased. The inner splitting, $2T_{\perp}$, broadened and the high field peak height of the inner hyperfine doublet (ie, peak 4 in Fig 1) decrease with increasing

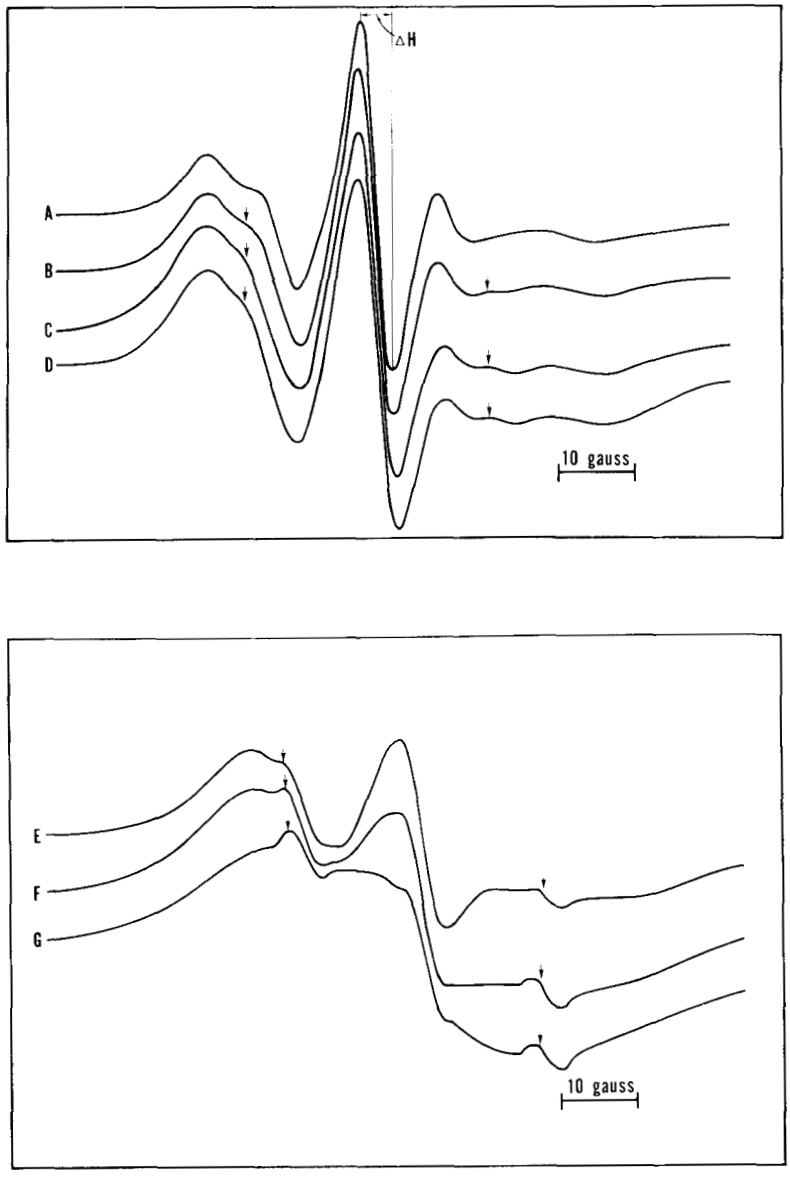

Fig 2. Unexpanded spectra of rat heart plasma membranes (37°C), labeled with varying I(12,3) probe concentrations. A – "Low" range spectrum of heart membranes labeled with 14 μg I(12,3)/mg protein; B, C, and D are "high"-range spectra of heart membranes labeled with 25, 46, and 53 μg I(12,3)/mg protein, respectively. The spectra in A–D were normalized so that the amplitudes of the central bands were equal; E, F, and G are "very high"-range spectra of heart membranes labeled with 88, 147, and 235 μg I(12,3)/mg protein, respectively. The low, high, and very high probe ranges are defined in the Results. Figure 2A indicates ΔH (the peak-to-peak distance of the central band). The positions of the "fluid" or "liquid-line" spectral components are indicated by arrows in Figure 2 B–G.

I(12,3) probe concentration; however, $2T_{\perp}$ could not be measured for concentrations exceeding approximately 88 μg I(12,3)/mg protein due to the unresolved inner doublet (see Figure 2E). The peak-to-peak distance of the central band (ie, ΔH in Figure 2A) similarly broadened with the probe concentration for the range 14–88 μg I(12,3)/mg protein. Figure 2F indicates that ΔH cannot be accurately measured for probe concentrations greater than approximately 147 μg I(12,3)/mg protein. In addition, the high-field baseline became depressed, whereas the low-field baseline became elevated with increasing probe concentration. Despite the presence of spectral changes in Figure 2 B–D, $2T_{||}$ was essentially constant throughout this probe concentration range; at higher probe/lipid ratios, the sloping baseline interfered with the measurement of the outer hyperfine splittings (see Figure 2 E–G. Last, a "fluid" or "liquid-line" spectral component appeared in addition to the immobilized spectrum in heart plasma membranes at the higher probe/lipid ratios Fig 2 B–G). Previous experiments have suggested that the "fluid" component is due to the partitioning of the I(m,n) probe into the aqueous environment [16, 19, 30]. Spectra qualitatively similar to those in Figure 2 A–E were obtained in earlier I(12,3) probe titrations of liver (31°C) and heart (22°C) plasma membranes [19].

The functional dependence of the order parameters S, $S(T_{||})$, and $S(T_{\perp})$ on the I(12,3) probe concentration was determined for heart (37°C) and liver (31°C) plasma membranes (Fig 3). The $S(T_{||})$ values were relatively independent of the probe concentrations used in Figure 3 to examine both membrane systems. However, S and $S(T_{\perp})$ decreased substantially if the I(12,3) concentration exceeded 25 or 1.5 μg/mg protein in heart and liver membranes, respectively; the decrease in $S(T_{\perp})$ was greater than the corresponding decrease in S. If the μg I(12,3)/mg protein ratios for heart and liver membranes were greater than 52 and 4, respectively, then S and $S(T_{\perp})$ could not be calculated due to the unresolved inner hyperfine doublet. As noted in a previous I(12,3) study of rat cardiac sarcolemma, the ESR signal from heart membranes decreased slightly with time for temperatures above 30°C [19]. Nevertheless, plots of S, $S(T_{||})$, and $S(T_{\perp})$ vs time indicated that the order parameters of cardiac sarcolemma (37°C) did not significantly vary after 2.5 h from initial values.

Several characteristic probe/lipid ratio ranges may accordingly be identified for liver (31°C) and heart (37°C) (Table I in [19] and Figs 2 and 3): (1) the "low" range was where ΔH, the hyperfine splittings $2T_{||}$ and $2T_{\perp}$, and the order parameters S, $S(T_{||})$, and $S(T_{\perp})$ were constant (independent of probe concentration). "Intrinsic" membrane properties may be determined from these spectra. A negligible fluid component was also associated with this range (Fig 3D in [19] and Fig 2A); (2) the "high" range was characterized by a broadening of $T_{\perp}$ and ΔH with increasing probe concentration and the appearance of a small fluid component (Fig 3E in [19] and Fig 2 B–D); $T_{||}$ was virtually unchanged from low-range values. Therefore, S and $S(T_{\perp})$ measured only an "apparent" fluidity in this range, whereas $S(T_{||})$ more nearly reflects a polarity-uncorrected, "intrinsic" membrane fluidity; and (3) the "very high" range was identified by noticeably broadened spectra and the presence of a substantial fluid component (Fig 3F in [19] and Fig 2 E–G). The measurement of ΔH and the hyperfine splittings was either difficult or impossible in this range because of the broadened spectra and sloping baseline. An interesting observation is that the onset of broadening in the spectra of heart membranes at 37°C occurred at much

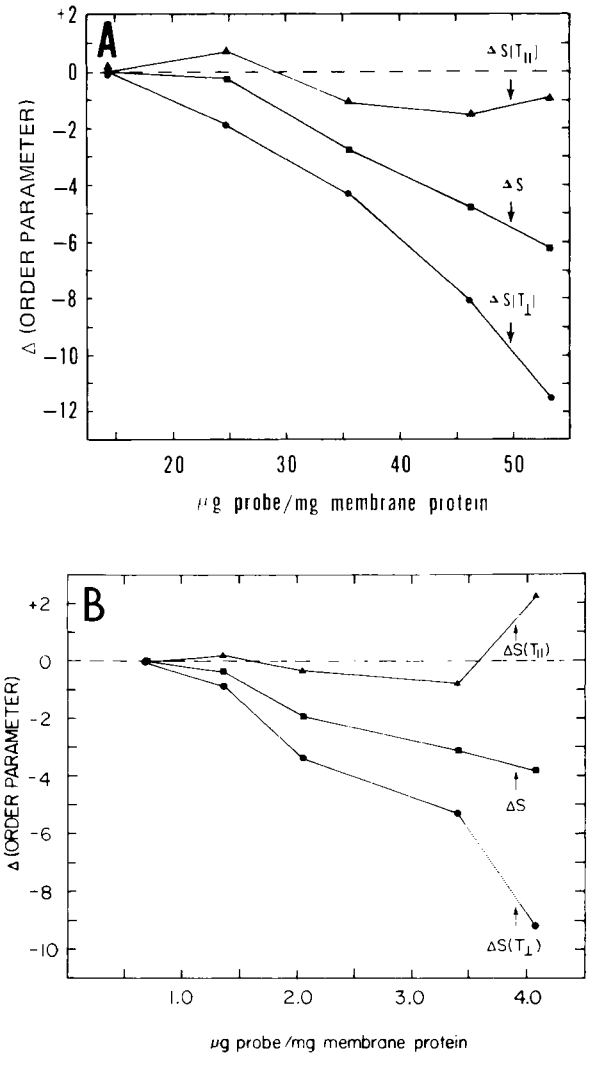

Fig 3. The effects of increasing I(12,3) probe concentration on the order parameters of heart (37°C) and liver (31°C) membranes. A – $\triangle S$, $\triangle S(T_{||})$ and $\triangle S(T_{\perp})$, the percent changes in the cardiac sarcolemmal order parameters from baseline values measured at 14 μg probe/mg protein, are plotted as a function of I(12,3) probe concentration. The control values of S, $S(T_{||})$, and $S(T_{\perp})$ are 0.580, 0.615, and 0.552. Low-range order parameters were calculated from heart membranes labeled with less than 20 μg I(12,3)/mg protein, whereas high-range order parameters were measured from heart membranes labeled with 25–53 μg probe/mg protein (see Results). The order parameters were determined using unexpanded spectra with magnified wings (see Materials and Methods); B – $\triangle S$, $\triangle S(T_{||})$ and $\triangle S(T_{\perp})$, the percent changes in the liver plasma membrane order parameters from baseline values measured at 0.7 μg probe/mg protein, are plotted as a function of the I(12,3) concentration. The control values of S, $S(T_{||})$, and $S(T_{\perp})$ are 0.614, 0.643, and 0.593. Low-range order parameters were calculated from liver membranes labeled with less than 1.4 μg I(12, 3)/mg protein, whereas high-range order parameters were measured for liver membranes labeled with approximately 1.4–4.1 μg probe/mg protein (see Results). S, $S(T_{||})$, and $S(T_{\perp})$ were calculated from expanded spectra as indicated in Materials and Methods.

higher probe/lipid ratios than those previously noted for liver (31°C) or heart (22°C) membranes (see Discussion).

It is important to determine why the spectra of labeled rat heart and liver plasma membranes are altered with increasing I(12,3) probe concentration. Clearly, extensive probe–probe interactions (ie, dipole–dipole and/or spin exchange interactions) occur in heart (Fig 2E–G) and liver (Fig 3F in [19]) membranes labeled with "very high" probe concentrations. Similarly broadened ESR spectra have been reported for other biological membranes when labeled with high I(m,n) probe concentrations [31–34]. Enhanced nitroxide radical interactions are also probably responsible for the "apparent" increase in the fluidities of heart and liver membranes observed with increasing probe concentration in the "high" range (Fig 3). For example, the broadening of $T_{\perp}$ was closely correlated with increases in ΔH for both membrane systems (see Fig 6 in [19]); other investigators have previously demonstrated that radical interactions can broaden the ΔH of labeled model [35, 36] and biological [31, 34, 37] membranes. The increase in $T_{\perp}$ was also associated with such characteristic exchange-broadened effects as the decrease in the high-field peak height of the inner hyperfine doublet [10, 38, 39] and the downward displacement of the high-field baseline (Fig 2 D–G and Fig 3F in [19]) [10, 16, 39, 40]. The observation that $T_{||}$ [and $S(T_{||})$] is essentially unaltered throughout the low and high ranges indicates that the "apparent" increase in fluidity with probe concentration is not the result of probe-mediated perturbations in the membrane structure; any fluidization that permits more flexibility in the membrane-incorporated probe requires that $2T_{||}$ commensurately decrease with increases in $2T_{\perp}$.

Temperature Effects on the Order Parameters of I(12,3)-Labeled Rat Heart and Liver Plasma Membranes

The temperature dependence of the various order parameters was determined from the spectra of heart plasma membranes containing a "low" I(12,3) probe concentration; Figure 4A shows that the $S(T_{||})$, S, and $S(T_{\perp})$ values of I(12,3)-labeled heart membranes (20 μg probe/mg protein) decrease with increasing temperature. A plausible interpretation of Figure 4A is that the I(12,3) probe becomes less flexible as the temperature is lowered. These results may also be used to infer that the flexibility (or "fluidity") of native lipids surrounding the probe is similarly sensitive to temperature alterations. Closer inspection of Figure 4A indicates the presence of a "break" at approximately 32°C for each order parameter vs $1/T(^{\circ}K)$ curve. These discontinuities suggest that an abrupt change in the environment of the probe occurs at 32°C, possibly due to either a lipid phase separation or transition. The slope of each order parameter vs $1/T(^{\circ}K)$ curve becomes steeper for temperatures above the break in the direction expected for decreased viscosity. Similar breaks have previously been identified in order parameter plots obtained from I(m,n)-labeled model [41], and biological [21, 31, 42] membranes and have also been attributed to either a phase separation or transition.

Nevertheless, the analysis of Arrhenius-type plots of order parameters such as Figure 4A might be complicated if probe–probe interactions were to occur in the membrane. Since the probe concentration employed in Figure 4A was not established as being "magnetically dilute" for each temperature in the range 8° to 35°C, the order parameters S and $S(T_{\perp})$ must be viewed as empirical parameters that are functions of not only the motion of the probe but also perhaps nitroxide radical interactions; $S(T_{\perp})$ is also a function

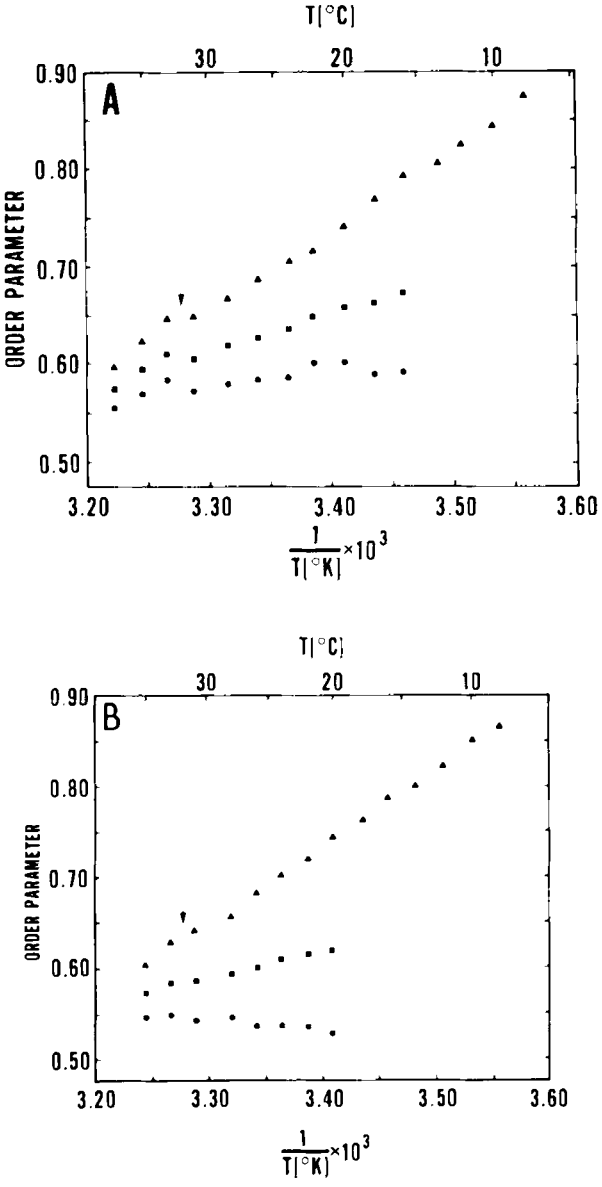

Fig 4. Temperature dependence of S (■—■), $S(T_{||})$ (▲—▲), and $S(T_{\perp})$ (●—●), where S (Eq 5), $S(T_{||})$ (Eq 1), and $S(T_{\perp})$ (Eq 2) were calculated from the spectra of I(12,3)-labeled heart plasma membranes. The hyperfine splittings, $2T_{||}$ and $2T_{\perp}$, were measured from unexpanded spectra with magnified wings (see Materials and Methods). A – Order parameters were determined from heart plasma membranes labeled with a low I(12,3) probe concentration (ie, 20 μg probe/mg protein). B – Order parameters were determined from heart plasma membranes labeled with a high I(12,3) probe concentration (ie, 45 μg probe/mg protein). The temperature range was approximately 8° to 37°C. Order parameters were calculated using $(T_{XX}, T_{ZZ}) = (6.1, 32.4)$ gauss [27]. The arrows indicate the apparent break temperature at 32°C (see Results and Discussion).

of the membrane polarity. However, $S(T_{||})$ is probably sensitive only to alterations in either the motion of the probe or the polarity of the environment of the probe. The breaks observed at 32°C in Figure 4A may not solely reflect changes in the lipid fluidity, but could also be the result of abrupt alterations in membrane polarity and/or probe–probe interactions induced by the lipid phase separation.

Figure 4A also indicates that the slopes of the order parameter vs $1/T(^{\circ}K)$ curves, obtained from heart membranes labeled with 20 μg I(12,3)/mg protein, become steeper in the following order: $S(T_{\perp}) < S < S(T_{||})$. Furthermore, the approximate and polarity-corrected order parameter curves appear to merge at approximately the break temperature, 32°C. The differences in the slopes of these curves might be accounted for if the polarity of the environment of the probe were to increase with decreases in temperature. An alternate interpretation for the divergence of these order parameter vs $1/T(^{\circ}K)$ curves is that probe–probe interactions increase as the temperature is lowered below 32°C. Consideration of only the data in Figure 4A is, unfortunately, insufficient to permit us to choose between these explanations.

The effects of temperature on the various order parameters were also examined with rat heart plasma membranes labeled with a "high" I(12,3) probe concentration (Fig 4B). The $S(T_{||})$ vs $1/T(^{\circ}K)$ curves obtained from heart membranes labeled with either a "low" (Fig 4A) or "high" (Fig 4B) probe concentration were generally in good agreement. However, the high range S and $S(T_{\perp})$ values of Figure 4B were considerably lower than the corresponding order parameters measured using a low probe/mg protein ratio for each temperature in the range 20° to 32°C. Although S and $S(T_{||})$ decreased with increasing temperature in Figure 4B, $S(T_{\perp})$ was observed to increase with increasing temperature. The anomalous behavior of the high range $S(T_{\perp})$ vs $1/T(^{\circ}K)$ curve may be due to enhanced nitroxide radical interactions that occur in heart membranes at lower temperatures. It should also be pointed out that the "discontinuity" at 32°C was less pronounced for each curve in Figure 4B.

Difference cardiac sarcolemmal order parameter vs $1/T(^{\circ}K)$ plots were also calculated as the percent difference between values obtained at high and low probe concentrations for each temperature. Figure 5 indicates that $\Delta S(T_{\perp})$ and ΔS become more negative for temperatures below 32°C, whereas $\Delta S(T_{||})$ did not vary significantly from zero for the range 8° to 32°C. The invariance of the outer splitting suggests that, for both low and high probe concentrations, the immobilized spectra reflect only those I(12,3) probe molecules that sample lipid domains sharing the same fluidity and polarity. Since it is reasonable to assume that the flexibility and polarity contributions to the low and high range $S(T_{\perp})$ values will be equal at a given temperature, $\Delta S(T_{\perp})$ (or, alternatively, $\Delta T_{\perp}$) may be an empirical parameter that reflects only nitroxide radical interactions. It should be recalled that $S(T_{\perp})$ decreased as the I(12,3) probe concentration increased in heart plasma membranes at 22° [19] and 37°C. The observation that $\Delta S(T_{\perp})$ in Figure 5 becomes more negative for temperatures below 32°C therefore suggests that lowering the temperature also promotes probe–probe interactions in heart membranes. A similar difference plot of ΔH vs $1/T(^{\circ}K)$, calculated from low and high range spectra, increased between 35° to 22°C, but plateaued between 8° and 21°C (data not shown). One interpretation of the above data is that a lipid phase separation in rat heart plasma membranes (between 21° and 32°C) induces a segregation of the I(12,3) probe, thereby increasing both the "effective" I(12,3)/lipid ratio and nitroxide radical interactions (see Discussion).

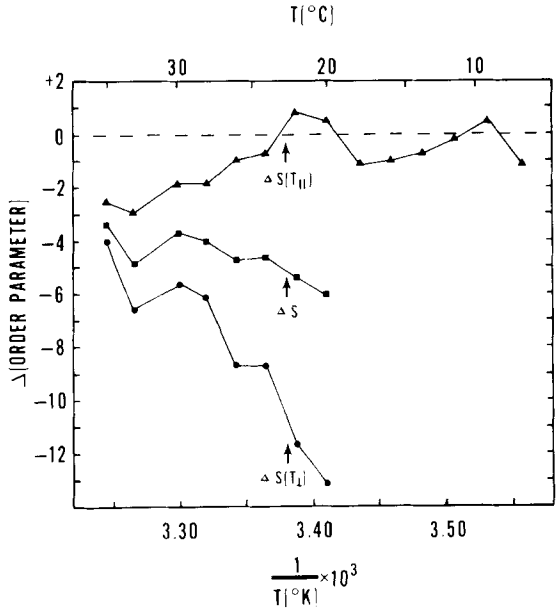

Fig 5. Temperature dependence of ΔS (■—■), $\Delta S(T_{||})$ (▲—▲), and $\Delta S(T_{\perp})$ (●—●), where Δ(order parameter) was calculated from rat heart plasma membrane at a given temperature as the percent difference between values measured at high (ie, the 45 μg I(12, 3)/mg protein ratio used in Figure 4B) and low (ie, the 20 μg I(12,3)/mg protein ratio used in Figure 4A) I(12,3) probe concentrations. S and $S(T_{\perp})$ values could not be measured for temperatures less than 20°C due to the poorly resolved inner hyperfine doublet in the high-range spectra. This plot was obtained by progressing from low to high temperatures; similar results were observed if spectra were measured by progressing from high to low temperatures.

The order parameters of I(12,3)-labeled rat liver plasma membranes were previously studied as a function of temperature. Plots of $(1 - S)/S$, $[1 - S(T_{||})]/S(T_{||})$ [19], and $[1 - S(T_{\perp})]/S(T_{\perp})$ (data not shown in [19]) vs $1/T(^{\circ}K)$ were obtained from liver membranes labeled with a probe concentration which was magnetically dilute at 31°C (0.7 μg I(12,3)/mg protein). These plots indicated the presence of characteristic breaks at 19° and 28°C. The discontinuities were also detected if higher probe concentrations (1.3 and 2.6 μg probe/mg protein) were employed. These spin-label studies suggested that a lipid phase separation occurs in liver plasma membranes between 19° and 28°C.

It is worthwhile to compare in more detail the order parameter vs $1/T(^{\circ}K)$ curves obtained from liver plasma membranes labeled with different I(12,3) probe/lipid ratios. The $S(T_{||})$ vs $1/T(^{\circ}K)$ curves of liver membranes labeled with either 0.7 or 2.6 μg probe/mg protein agreed, in general, throughout the temperature range 35° to 22°C. However, the S and $S(T_{\perp})$ values of liver membranes labeled with 2.6 μg probe/mg protein were lower than the corresponding order parameters of liver membranes containing 0.7 μg probe/mg protein for temperatures less than 27°C. Figure 6 shows that $\Delta S(T_{\perp})$ and ΔS become more negative for temperatures below approximately 27°C, whereas $\Delta S(T_{||})$ did not significantly vary from zero. The use of temperatures below 27°C apparently increases probe–probe inter-

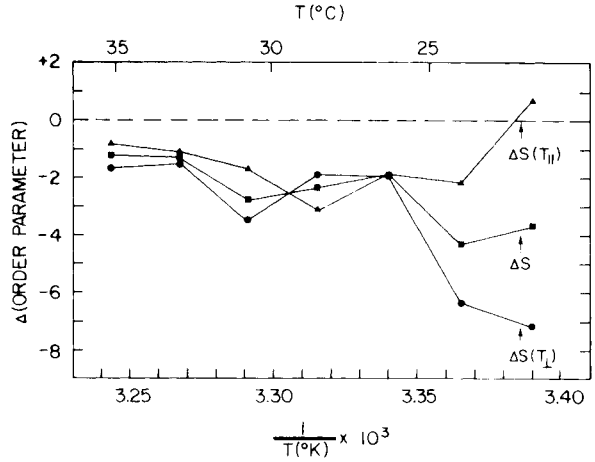

Fig 6. Temperature dependence of △S(■—■), △S($T_{||}$) (▲—▲), and △S($T_{\perp}$) (●—●), where △(order parameter) was calculated from rat liver plasma membrane at a given temperature as the percent difference between values measured at 0.7 and 2.6 μg I(12, 3)/mg protein ratios. Hyperfine splittings were determined from expanded spectra on a Varian E-3 ESR spectrometer as described elsewhere [19]. The temperature range was 21° to 35°C.

actions in liver plasma membrane, inasmuch as I(12,3) probe additions at 31°C to liver membranes decreased S($T_{\perp}$) and S, whereas S($T_{||}$) was unaffected (Fig 3B). These preliminary data suggest that a lipid phase separation occurs in rat liver plasma membrane between 19° and 28°C, which induces a segregation of the I(12,3) probe for temperatures below 27°–28°C.

Ca^{2+} Effects on the Fluidities of Rat Heart and Liver Plasma Membranes

The effects of Ca^{2+} on the spectra of I(12,3)-labeled cardiac sarcolemma (14 μg probe/mg protein) were studied at 37°C. Titrations of the sarcolemma were performed with successive additions of $CaCl_2$. As may be seen in Table I, mM $CaCl_2$ decreased the sarcolemmal fluidity, as indicated by positive increases in ΔS, Δ S($T_{||}$) and Δ S($T_{\perp}$). The calcium effect on the fluidity was apparently a concentration-dependent saturable process reaching a plateau at about 2.2 mM. The use of "saturating" concentrations of $CaCl_2$ increased S by approximately 4.7%; a decrease in the membrane temperature from 37° to 32°C would be necessary to increase S by a similar amount. Furthermore, the decrease in heart membrane fluidity mediated by 3.2 mM $CaCl_2$ could be reversed by 27 mM EGTA. Control experiments indicated that addition of 27 mM EGTA, or 27 mM EGTA premixed with 3.2 mM $CaCl_2$, did not affect the fluidity of untreated heart plasma membranes. The spectral alterations induced by Ca^{2+} were not simply due to an ionic strength effect, inasmuch as 9.5 mM NaCl (or 9.5 mM KCl) did not change the S of heart membranes [23].

TABLE I. Effects of $CaCl_2$ on the Order Parameters* of I(12,3)-Labeled Rat Heart and Liver Plasma Membranes† at 37°C

$CaCl_2$ (mM)	$S(T_{\|})$	$\Delta S(T_{\|})$	$S(T_{\perp})$	$\Delta S(T_{\perp})$	S	ΔS
Heart plasma membrane						
0.0	0.615	–	0.548	–	0.578	–
0.6	0.624	1.5	0.565	3.1	0.591	2.2
1.2	0.631	2.6	0.560	2.2	0.591	2.2
1.7	0.630	2.4	0.568	3.6	0.596	3.1
2.2	0.638	3.7	0.572	4.3	0.601	3.9
3.2	0.642	4.3	0.578	5.3	0.606	4.7
Liver plasma membrane						
0.0	0.585	–	0.564	–	0.573	–
1.0	0.602	2.9	0.572	1.4	0.586	2.2
2.0	0.614	4.8	0.577	2.3	0.593	3.4
2.8	0.615	5.0	0.587	4.0	0.599	4.4
3.9	0.623	6.3	0.584	3.5	0.601	4.8

*Order parameters were calculated as indicated in the text. The hyperfine splittings, $2T_{\|}$ and $2T_{\perp}$, of liver plasma membranes were measured from expanded spectra (see [19, 26]), whereas the corresponding splittings of heart plasma membranes were determined from "unexpanded spectra with magnified wings" (see Materials and Methods); the 0.8 gauss addition to the apparent $T_{\perp}$ value is included [15]. Δ (order parameter) was calculated as the percent difference between values measured with and without calcium.

†Liver and heart membranes were labeled with 0.7 and 1.4 μg I(12,3) per mg protein.

Calcium-induced alterations in the fluidity of I(12,3)-labeled rat liver plasma membranes (0.7 μg probe/mg protein) were also determined from expanded spectra at 37°C. Addition of mM $CaCl_2$ decreased the liver membrane fluidity, as indicated by positive increases in ΔS, $\Delta S(T_{\|})$ and $\Delta S(T_{\perp})$ (Table I). This confirms the results of a previous study which examined the effects of $CaCl_2$ on the unexpanded spectra of I(12,3)-labeled liver plasma membranes [21]. The effects of $CaCl_2$ on the fluidity of liver membranes may also be viewed as a concentration-dependent saturable process in which the plateau is reached at approximately 2.8 mM. The maximum positive increase in the S of I(12,3)-labeled liver membranes induced by saturating concentrations of $CaCl_2$ was 4.8%; a similar increase in S may be obtained by lowering the membrane temperature from 37° to 31°C [19].

The interpretation that Ca^{2+} decreases the fluidities of I(12,3)-labeled liver and heart plasma membranes must, however, be viewed with caution since Ca^{2+} has also been shown to segregate spin probes in several model membranes [10, 16, 39]. Any Ca^{2+}-induced changes in the fluidity could conceivably be obscured if enhanced probe–probe interactions were simultaneously to perturb the calculated order parameter [19]. Nevertheless, probe segregation was judged here to be unimportant, since the ESR spectra of Ca^{2+}-treated liver and heart membranes did not exhibit significant exchange broadening. Moreover, the functional relationship between Ca^{2+}-mediated alterations in the hyperfine splittings and the probe/lipid ratio was examined in I(12,3)-labeled heart plasma membranes following a previously described protocol [19]. The alterations in S, $S(T_{\|})$, and $S(T_{\perp})$ induced by

TABLE II. Effects of $LaCl_3$ on the Order Parameters* of I(12,3)-Labeled Rat Heart Plasma Membranes† at 37°C

$LaCl_3$ (μM)	$S(T_{\|})$	$\Delta S(T_{\|})$	$S(T_{\perp})$	$\Delta S(T_{\perp})$	S	ΔS
0	0.597	–	0.529	–	0.560	–
24	0.605	1.3	0.538	1.7	0.568	1.4
48	0.614	2.8	0.547	3.3	0.576	2.8
101	0.628	5.1	0.564	6.4	0.592	5.6
149	0.632	5.7	0.558	5.3	0.590	5.2
192	0.655	9.3	0.555	4.8	0.598	6.6

*Order parameters were calculated as indicated in the text. The hyperfine splittings, $2T_{\|}$ and $2T_{\perp}$, were measured from "unexpanded spectra with magnified wings" (see Materials and Methods); the 0.8 gauss addition to the apparent $T_{\perp}$ value is included [15]. Δ(order parameter) was calculated as the percent difference between values measured with and without lanthanum.
†Heart membranes were labeled with 14 μg I(12,3) per mg protein.

saturating concentrations of Ca^{2+} were independent of whether the heart membranes contained low or high probe concentrations [23]; this suggests that cation-mediated changes in radical interactions do not occur. The most reasonable explanation of the above Ca^{2+} effects on liver and heart plasma membrane ESR spectra is that Ca^{2+} ions decrease the flexibility of the membrane-incorporated spin probe by binding to specific sites.

$LaCl_3$ Effects on the Fluidity of Rat Heart Plasma Membranes

$LaCl_3$ was also tested for its effects on the spectra of I(12,3)-labeled cardiac sarcolemma at 37°C. Table II shows that successive μM $LaCl_3$ additions decreased the lipid fluidity, as indicated by increases in S, $S(T_{\|})$, and $S(T_{\perp})$. The lanthanum effects on heart plasma membrane fluidity may be described as a concentration-dependent saturable process similar to that observed with Ca^{2+}, although here the plateau was reached at approximately 150 μM $LaCl_3$. It should be noted that the magnitude of the La^{3+} effect on the membrane fluidity was greater and occurred at lower concentration than that induced by Ca^{2+}; for example, addition of 192 μM $LaCl_3$ or $CaCl_2$ increased S by 6.6 or 1.0%. Furthermore, the increase in S mediated by 192 μM La^{3+} was only partially reversed by 27 mM EGTA. The ΔS, $\Delta S(T_{\|})$ and $\Delta S(T_{\perp})$ values, obtained upon addition of a saturating La^{3+} concentration, did not depend on the probe concentration for probe/lipid ratios selected from the low and high ranges [23]. La^{3+} probably alters the ESR spectra of I(12,3)-labeled cardiac sarcolemma by binding to specific membrane sites, thereby decreasing the fluidity of the lipid bilayer.

DISCUSSION

The Effects of I(12,3) Probe Concentration on Membrane ESR Spectra and Calculated Order Parameters

It seems likely that the order parameter effects and spectral alterations observed upon increasing the I(12,3) probe concentration in liver and heart plasma membranes are due to enhanced probe–probe interactions. Certainly, the "very high" range spectra for

heart (37°C) (Fig 2G) and liver (31°C) (not shown) membranes predominately feature single broad lines that are characteristic of extensive nitroxide radical interactions. The two types of probe–probe interactions which may affect the ESR spectra of labeled membranes are dipole–dipole and spin–exchange [36]. Exchange interactions are due to the exchange, or "flip-flop," of the spin states of two neighboring radicals having oppositely oriented spins. This electronic interaction requires that the participating nitroxide groups be essentially in van der Waal's contact and decreases rapidly as the distance between the radicals increases. Therefore, the exchange process for dilute solutions of radicals not only depends on the label concentration but also is diffusion-controlled. On the other hand, dipole–dipole interactions are relatively long-range effects that tend to be averaged out in the presence of rapid diffusion and/or tumbling; these effects occur when the magnetic moments of nitroxide radicals produce local magnetic fields that may superimpose with the externally applied magnetic field at sites of other radicals. Both dipole–dipole and spin-exchange interactions may be involved in the spectral broadening observed in Figure 2, although the relative contributions cannot be assessed from an examination of only the very high range spectra.

Two distinct physical models are proposed to account for spectra obtained from liver (31°C) and heart (37°C) plasma membranes labeled with low, high, and very high I(12,3) probe concentrations:

The uniform distribution model. Here, the I(12,3) probe is viewed as being homogeneously dispersed throughout the accessible lipid domains for the entire probe concentration range. Experimental evidence provided earlier suggests that those liver (31°C) and heart (37°C) plasma membrane lipid domains sampled by the I(12,3) probe are in a liquid or disordered state. Thus, the I(12,3) probe intercalates into liquid lipids at low probe concentrations, presumably without perturbing the lipid phase. In the high probe concentration range, all of the membrane-incorporated I(12,3) probe molecules participate in nitroxide radical interactions which not only broaden ΔH and $2T_{\perp}$ but also decrease S and $S(T_{\perp})$. The spectral broadening noted in the high range is probably due to weak exchange interactions, since the I(12,3) probe undergoes rapid anisotropic motion which tends to diminish dipole–dipole interactions. The uniform distribution model also predicts that the exchange process will be diffusion-controlled for dilute solutions of the spin label. It should, in principle, be possible to evaluate the lateral diffusion constant for the membrane-incorporated probe if this model is valid; however, a major uncertainty in the estimation of such diffusion constants concerns the size of the lipid pool in which the I(12,3) probe is soluble. The observation that $2T_{||}$ and $S(T_{||})$ remain virtually unchanged in the high range suggests that the use of these probe concentrations alters neither the polarity nor the fluidity of the environment of the probe. It should also be noted that the exchange process will not be necessarily diffusionally-limited at the highest probe/lipid ratio in Figure 2, since here the average distance between pairs of labels may be closer than the "critical radius" for spin exchange [43].

The patch model. In this model, the membrane contains only a limited number of binding sites in the lipid matrix that can be occupied by the I(12,3) probe. The low probe concentration spectra accordingly reflect the environment of the I(12,3) probe in these sites. As the I(12,3) probe concentration increases and these sites become filled, a phase of pure (or, at least, very concentrated) I(12,3) molecules may then coexist with the endogenous lipids as segregated "patches." The high range spectra would therefore consist of two spectral components: (1) An anisotropic, immobilized spectrum which reflects magnetically dilute probe molecules occupying membrane sites; and (2) a single broad line

(eg, similar to Figure 2G) which represents I(12,3) probe existing in concentrated patches. Only those I(12,3) molecules in the patches would contribute to the nitroxide–radical interaction broadening observed in the high range. The absence of a marked probe concentration effect on $2T_{||}$ in the high range suggests that these segregated patches do not perturb the environment of the I(12,3) probe bound to membrane sites. An important consequence of the patch model is that it should not be possible, even in principle, to use high range spectra to calculate diffusion constants for the membrane-incorporated probe.

Next one should consider how well the above models account for the low, high, and very high probe range spectra of heart and liver membranes. The patch model readily explains such high probe range spectral alterations as the broadening in $2T_{\perp}$ and ΔH, the decrease in the high-field peak height of the inner hyperfine doublet, and the depression in the high-field baseline. Each of the above spectral changes would be predicted if a single broad line arising from concentrated patches of I(12,3) probe were to be centered over the anisotropic spectrum of probe molecules residing in membrane sites; progressive increases in the I(12,3) probe concentration would be expected to increase both the proportion of probe molecules in the segregated domains and the magnitude of the broad line that contributes to the membrane ESR spectra. The patch model is also consistent with the observation that $2T_{||}$ is constant in the high probe range, since here the single broad line should have relatively little influence on the outermost peaks. Moreover, increasing the proportion of probe in the segregated patches would not necessarily affect the behavior of I(12,3) probe occupying membrane sites since the patch model requires the coexistence of distinct probe-containing phases. It should be noted that a phase of pure phospholipid spin label was previously found to separate out at temperatures below 20°C in sarcoplasmic reticulum [37]. Furthermore, clusters of androstane spin probe were detected in a spin-label study of dipalmitoyl lecithin (DPL) at temperatures below the phase transition [44].

The uniform distribution model does not explain the spectra of I(12,3)-labeled liver and heart plasma membranes as readily as does the patch model. For example, a rather complicated mechanism involving "weak exchange" interactions would have to be invoked for the former model to account for high-range spectral changes. Additional studies must, however, be performed in order to determine which model more accurately reflects the distribution of I(12,3) in the membrane. It is also possible that the use of very high probe concentrations may greatly perturb the structures of liver or heart membranes, and in such cases neither the patch nor the uniform distribution model would be expected to describe faithfully the structure of the labeled membrane.

Determination of Lipid Phase Separations From Liver and Heart Plasma Membrane ESR Spectra

Plots of $S(T_{||})$, S and $S(T_{\perp})$ vs $1/T(^{\circ}K)$, obtained from I(12,3)-labeled heart and liver plasma membranes, were examined for the presence of phase separations (or transitions) that might alter the flexibility of the membrane-incorporated probe. Characteristic breaks or discontinuities occurred in heart plasma membranes at 32°C and also in liver plasma membranes at 28° and 19°C. Such breaks might signal the onset of phase changes in the respective plasma membrane lipids sampled by the probe.

However, the assignment of phase separations from order parameter vs $1/T(^{\circ}K)$ curves is not particularly straightforward. One serious problem is that probe–probe interactions might interfere with the detection of characteristic breaks in such plots. For example, the 32°C break in order parameter vs $1/T(^{\circ}K)$ plots of heart membranes is probably less pronounced in Figure 4B than in Figure 4A because of enhanced radical interactions. Further-

more, probe–probe interaction effects may obscure the existence of a low-temperature break in Figure 4A or B, inasmuch as the use of low temperatures in I(12,3)-labeled heart membranes promotes radical interactions. The absence of a low characteristic temperature in Figure 4 is particularly anomalous, in view of the $\Delta(\Delta H)$ vs $1/T(^{\circ}K)$ plot which suggested a low-temperature end to the phase separation at approximately 20°C. Perhaps similar probe–probe interactions occurred at lower temperatures in a previous study of I(12,3)-labeled rat liver plasma membranes (probe:phospholipid equal to 1:100) thereby permitting Houslay et al [45] to detect only the 28.5°C break and not the additional discontinuity we observed at 19°C [19]. A second difficulty in interpreting Arrhenius-type plots of order parameters concerns the distribution of the probe in the membrane. I(m,n) labels have been found to partition preferentially into the more fluid phase [16–18, 46]. If the I(12,3) probe should be restricted to the more liquid lipid domains (L), phase changes occurring in the solid lipid domains (S) will not necessarily be detected in order parameter vs $1/T(^{\circ}K)$ plots.

Empirical parameters that primarily reflect probe–probe interactions were also employed in order to observe lipid phase separations in I(12,3)-labeled liver and heart plasma membranes. The temperature dependence of radical interactions in these membranes was studied with Δ(order parameter) (Figs 5 and 6) and $\Delta(\Delta H)$ vs $1/T(^{\circ}K)$ plots. Lowering the temperature appears to promote probe–probe interactions in heart (from 32° to 21°C) or liver (from 27° to 20°C) plasma membranes, since $\Delta S(T_{\perp})$ vs $1/T(^{\circ}K)$ plots of these membranes became more negative within the above temperature range. Unfortunately, these Δ(order parameter) plots could not be used to assess probe–probe interactions below 20°C, inasmuch as $2T_{\perp}$ was unmeasurable due to the poorly defined inner hyperfine doublet. Last, a $\Delta(\Delta H)$ vs $1/T(^{\circ}K)$ plot obtained from I(12,3)-labeled heart plasma membranes indicated that radical interactions increased between 35° and 22°C, but plateaued between 8° and 21°C.

One interpretation of the above temperature data is that S forms within the fluid lipid matrix of liver (at 28°C) or heart (32°C) membranes which tend to segregate the I(12,3) probe. As the fraction of S increases with decreases in temperature, the proportion of clustered probe rises, leading to enhanced radical interactions. These lipid phase separations are easily reconciled with either of the proposed membrane-incorporated probe distribution models. The uniform distribution model might be used to predict that the I(12,3) probe was homogenously dispersed in L and did not partition into S; lowering the temperature, which decreases the proportion of L to S, would be expected to increase both the I(12,3) probe concentration in L and radical interactions. The patch model similarly predicts that the probe would be excluded from S; here, however, the formation of S will reduce the number of probe–membrane binding sites present in L, thereby increasing the proportion of pure phase probe. In the case of heart plasma membranes, the membrane-incorporated I(12,3) probe undergoing anisotropic motion probably remains soluble in a constant minimum fraction of lipid for temperatures less than 21°C, inasmuch as radical interactions do not change from 21° to 8°C.

The hypothesis that lowering the temperature forms concentrated domains of I(12,3) probe in liver and heart membranes is consistent with the results of previous spin-label studies. The onset of radical interactions in heart membranes occurred at lower probe concentrations at 22°C than at 37°C (ie, 1.5 vs 25 μg probe/mg protein) [19]; these results would be expected if the size of the membrane lipid domains sampled by the probe was much smaller at the lower temperature. Moreover, the use of temperatures below 20°C has been shown to promote radical interactions and probe clustering in DPL labeled with

an oxazolidine derivative of androstane [36], and also in sarcoplasmic reticulum probed with a phospholipid spin label [37].

The Nature of Thermotropic Lipid Phase Separations That Occur in Rat Liver and Heart Plasma Membranes

It is worthwhile to consider in more detail the lipid phase separation of liver plasma membranes. The breaks at 19° and 28°C observed in order parameter vs 1/T(°K) plots of I(12,3)-labeled liver membranes [19], as well as enhanced radical interactions that occur at temperatures less than 28°C, might suggest the following phase separation model. The 19°C break corresponds to a $S \longrightarrow S + L$ transition, whereas the 28°C break detected by ourselves and Houslay et al [45] reflects a $S + L \longrightarrow L$ transition. Recent 90° light scattering experiments of liver plasma membranes have provided additional evidence that a phase separation occurs at 28°C [47]. However, the preceding model is not entirely consistent with an electron diffraction study of frozen and thawed liver plasma membranes [48]. Hui and Parsons reported the presence of separate lipid phases only at temperatures less than 17.5°C; here, the diffraction patterns showed a faint but sharp ring at a spacing of 4.1 Å (indicating *S*) plus a faint diffuse band at a spacing of 4.6 Å (indicating *L*). Although the 17.5°C transition may be responsible for the characteristic temperature detected in our spin-label studies of liver plasma membranes at 19°C, Hui and Parsons attributed their transition to a $S + L \longrightarrow L$ transition rather than to $S \longrightarrow S + L$. Furthermore, the electron diffraction study of liver plasma membranes indicated that only *L* exists above 17.5°C and that no characteristic temperature occurs at 28°C [48].

A more complicated liver plasma membrane phase separation model is apparently required in order to reconcile the electron diffraction, spin-label, and 90° light scattering studies. One explanation is that *S* and *L* coexist at temperatures less than approximately 19°C; the anisotropic, immobilized spectra of I(12,3)-labeled liver plasma membranes at these low temperatures presumably reflect probe residing in *L*. The 19°C break would then correspond to *S* and *L* being dispersed into "quasi-crystalline" clusters (*QCC*) and *L*. Here, *QCC* are defined as having a packing density and fluidity in between that of *S* and *L*. Electron diffractographs of liver membranes would not necessarily be sensitive to *QCC* for several reasons. The presence of any diffraction band(s) arising from *QCC* (ie, bands probably having a spacing between 4.1 Å and 4.6 Å) might well be obscured by diffraction bands due to either the grid holding the membranes or *L*. Furthermore, the intensity of the faint 4.1 Å diffraction ring appears to be nonexistent along certain portions of its circumference (Fig 3 in [48]); it is not surprising that a diffraction band characteristic of *QCC*, which must be more diffuse than the 4.1 Å band, could not be detected by Hui and Parsons. If the solubility of the I(12,3) probe in *QCC* was low, then these clusters may be involved in the segregation of the probe which occurs at temperatures below 28°C in liver plasma membranes. The percentage of *QCC* will decrease with increases in temperature above 19°C until the 28°C transition is reached and the remaining *QCC* are converted into *L*. Although *QCC* may similarly coexist with *L* in heart plasma membranes between 21° and 32°C, additional studies must be performed before making such an assignment.

The presence of heterogeneous lipid phases in several model membranes at temperatures well above the classical gel $\longrightarrow$ liquid crystalline transition has been inferred from physical biochemical studies. Lee et al [5] suggested that the temperature-dependent partitioning of Tempo into DOL was affected by short-lived *QCC* below 30°C (ie, approximately 50°C above the phase transition); furthermore, Arrhenius plots of the motion of

DOL-incorporated spin [5] or fluorescent [49] probes yield discontinuities at approximately 30°C, consistent with the concept that distinct lipid phases occur below the break temperature. Studies on the temperature-dependent binding of N-phenyl-1-naphthylamine to egg lecithin liposomes [50] suggested the existence of "short-range order" for temperatures above the broad phase transition region of −15° to −5°C; moreover, the motion of various fluorescence probes incorporated into egg lecithin exhibited Arrhenius plots with deviations from linearity at approximately 35°C [49]. Last, several model membrane studies indicate that cholesterol may preferentially associate with specific lipids, thereby creating domains of differing fluidities. Phillips and Finer proposed that short-lived 1:1 lipid:cholesterol complexes are formed in lecithin:cholesterol mixtures; mixed lecithin–cholesterol bilayers with less than equimolar concentrations of cholesterol were predicted to consist of both free lipid and 1: 1 lipid:cholesterol complexes [7]. The Phillips and Finer model is consistent with recent results obtained from fluorescence [51] and electron diffraction [52] studies on DPL-cholesterol mixtures. These model membrane studies support the hypothesis that distinct lipid domains of differing fluidities may exist in both liver (between 19° and 28°C) and heart (between 21° and 32°C) plasma membranes. One possibility that should be explored is that the thermotropic phase separations that occur in liver and heart plasma membranes involve a redistribution of cholesterol, particularly in view of the high cholesterol/phospholipid ratios in these membranes [53, 54].

The Role of Thermotropic Lipid Phase Separations in the Expression of Liver and Heart Plasma Membrane Functions

The lipid phase separation that occurs between 19° and 28°C may affect a variety of liver plasma membrane-associated functions. For example, Terris and Steiner reported that the rate at which ^{125}I-insulin is degraded by isolated rat hepatocytes is negligible at temperatures of 0° to 20°C but rises rapidly between 20° and 30°C; these authors suggested that a lipid phase transition was responsible for this behavior [55]. Furthermore, studies conducted by Baur and Heldt indicate that Arrhenius plots of the glucose transport rate of rat hepatocytes exhibit an abrupt change at 18°C [56]. Both of these liver plasma membrane functions might be altered by the onset of the phase separation at 19°C.

The phase separation may also play an important role in regulating the activities of a number of liver plasma membrane enzymes. Arrhenius plots of the enzymatic activities of hormonal-stimulated adenylyl cyclase (AC), 5′-nucleotidase, Na^+,K^+- and Mg^{2+}-ATPase each exhibited breaks in the range 26–32°C [57–59]. It is possible that the end of the phase separation at 28°C dramatically influences the functioning of the above enzymes. In further studies, Houslay et al [57] measured the temperature-activity profiles of three classes of liver plasma membrane enzymes: (1) glucagon-stimulated AC (GSAC) and Na^+,K^+-ATPase, which span the width of the bilayer; (2) 5′-nucleotidase and Mg^{2+}-ATPase, which have active sites on the outer surface of the membrane; and (3) fluoride-stimulated AC (FSAC) and cAMP phosphodiesterase, which are confined to the inner half of the bilayer. Enzymes that were associated in some way with the outer half of the membrane exhibited breaks in Arrhenius plots between 25° and 30°C, whereas linear Arrhenius plots were obtained for enzymes localized on the inner surface. Accordingly, Houslay et al [57] proposed that these breaks were the result of a phase separation that occurs only in the outer half of the bilayer. The above data also suggest that the phase separation we detect in I(12,3)-labeled liver plasma membranes may be restricted to the outer half of the membrane.

The observation that Arrhenius plots of glucagon- (or epinephrine-) stimulated AC activity are biphasic with breaks at approximately 30°C, whereas the corresponding plots of FSAC are linear, indicates that the lipid state may affect the hormonal activation of AC [57, 58]. Cuatrecasas has recently proposed a "mobile receptor" model, which suggests that the lipid fluidity may play an important role in the hormonal stimulation of AC. The unliganded hormone membrane receptor (R) is viewed here as not being physically associated with AC [60]. The binding of the hormone (H) to R creates a hormone-receptor (H·R) complex that may now interact with AC. Both AC and H·R are presumed to be relatively free to diffuse laterally in the plane of the membrane, so that the rate of formation of the hormone–receptor–AC complex (H·R·AC) depends not only on the concentrations of H·R and AC, but also, perhaps, on the fluidity of the lipid domains. Houslay et al [57] suggested that the coupling of the glucagon receptor complex to AC renders the catalytic unit sensitive to the phase separation that occurs in the outer half of the bilayer. Furthermore, the lipid environment of liver plasma membranes was manipulated by substituting synthetic phosphatidylcholines for the native phospholipids. The break at 28.5°C, which was observed in Arrhenius plots of GSAC activity in native membranes, was shifted upwards by DPL, downwards by dimyristoyl lecithin, and was abolished by DOL; however, the Arrhenius plots of FSAC obtained from these altered membranes remained linear [57]. These studies further support the contention that the lipid fluidity is involved in the hormonal stimulation of AC.

The temperature dependence of various functional properties of mammalian myocardial preparations may be affected by a lipid phase separation similar to that observed between 21° and 32°C in rat cardiac sarcolemma. The permeability of the sarcolemma to various cations might be sensitive to the fluidities of the constituent lipid domains in view of the enhanced permeability of DPL liposomes to Na^+ that occurs as the lipid progresses from the gel to the liquid crystalline phase [61]. Moreover, Fossett and co-workers suggested that the sharp increase in the veratridine-stimulated uptake of $^{22}Na^+$ and $^{45}Ca^{2+}$ by cultured chick heart cells, which occurs upon raising the medium temperature from 25° to 32°C, might be caused by a lipid phase change in the plasma membrane [62]. Phase separations have also been implicated in the nonlinear Arrhenius plots of Na^+,K^+-ATPase activity obtained from plasma membrane preparations of rabbit heart (break at 20°C) [63] and kidney (break at 20°C) [42] and rat liver (see above) [57]. Consequently, the sarcolemmal lipid phase separation may, by influencing the permeability of the membrane to ions and the Na^+,K^+-ATPase activity, be associated with the temperature-induced alterations in the magnitude of the resting membrane potential and the nature and time course of the action potential [64]. Thus, the decrease in heart rate and increase in the isometric force of the heart that accompanies temperature reductions within the range 37° to 20°C [65] may indirectly be affected by the phase separation reported here between 21° and 32°C. Last, the presence of distinct lipid domains in heart plasma membranes might affect the hormonal stimulation of AC in a manner similar to that noted for liver plasma membranes. This prediction is supported by the observation that decreasing the temperature from 31° to 18°C dramatically inhibits the contractile response of rat left atrium to the AC activating, beta adrenergic agonist isoproterenol [66].

It is of particular interest that Arrhenius plots of several liver and heart plasma membrane functions are biphasic, with breaks corresponsing to either the onset or the ending of the respective lipid phase separations. For example, liver plasma membrane functions such as glucose transport and insulin degradation are greatly influenced by the low-temperature

break at 19°C, whereas liver membrane enzymes such as 5′-nucleotidase, GSAC, Mg^{2+}- and Na^+,K^+-ATPase are more affected by the 28°C break. It seems likely that the ability of a plasma membrane process to sense either the low- or high-temperature break critically depends on the location of the function vis à vis the various lipid domains.

We wish to emphasize that merely because a given membrane function demonstrates nonlinear Arrhenius plots with breaks at temperatures coincident to the onset or ending of the phase separation does not establish the lipid fluidity as having a regulatory role. Abrupt alterations in the activation energy of an enzyme, for example, might only be due to a temperature-sensitive protein conformation change which is independent of the membrane lipids [67]. Therefore, additional studies must be performed to ascertain the influence (if any) of the fluidity on a specific membrane function. One experimental approach would be to examine the expression of a given membrane functional property after the lipid composition of the membrane has been altered. Extensive studies have already employed this procedure to indicate that lipids play an important role in the hormonal activation of AC [57, 68--70]. The question of whether a membrane function is sensitive to the lipid state may also be tested with agents that are known to modulate the membrane fluidity. Of course, parallel studies on these perturbed membranes employing physical-biochemical techniques may serve to elucidate the structural basis for any functional alteration.

Interaction of Ca^{2+} and La^{3+} With Plasma Membranes: Effects on Lipid Fluidity

Ca^{2+} additions are reported here to increase the order parameters of I(12,3)-labeled liver and heart plasma membranes at 37°C in a concentration-dependent, saturable, and reversible manner. These results may be compared with previous $^{45}Ca^{2+}$-binding studies of rat liver and heart plasma membranes in which Scatchard plots revealed the presence of low- and high-affinity binding sites. The association constants for low-affinity sites were $5.6 \times 10^2 M^{-1}$ for rat cardiac sarcolemma [71] and $3.2 \times 10^2 M^{-1}$ for rat liver plasma membrane [72]. We suggest that the Ca^{2+}-induced rigidization of the membranes, which plateaus at 2.8 mM for liver and 2.2 mM for heart plasma membranes, may be mediated by the binding of Ca^{2+} to specific, low-affinity sites.

Earlier studies have shown that plasma membrane components such as proteins, phospholipids, and neuraminic acid are able to bind Ca^{2+}. For example, Shlatz and Marinetti [72] treated rat liver plasma membrane with phospholipases, neuraminidase, and proteases and demonstrated that acidic phospholipids and neuraminic acid play important roles in the binding of $^{45}Ca^{2+}$ to low-affinity sites. $^{45}Ca^{2+}$ binding to rat cardiac sarcolemma was also inhibited by similar enzymatic treatments [71]. Therefore, Ca^{2+}-mediated decreases in both liver and heart plasma membrane fluidities might be the result of cation interactions with endogenous phospholipids and/or neuraminic acid residues.

We also report that La^{3+} decreases the fluidity of I(12,3)-labeled heart plasma membranes in a concentration-dependent, saturable process. One possibility that should be explored is that these fluidity effects are mediated by the binding of La^{3+} to Ca^{2+} sarcolemmal binding sites. La^{3+} has been widely employed as a probe of Ca^{2+} membrane binding sites, in part because it associates with these sites less reversibly than does Ca^{2+}. The strong binding of La^{3+} to negatively charged, Ca^{2+} membrane sites would be expected since the hydrated radius of La^{3+} (3.1 Å) is similar to that of Ca^{2+} (2.8 Å) [73]. The results presented here indicate that La^{3+} also exhibits high affinity for those cardiac sarcolemmal sites which regulate the lipid fluidity; the La^{3+}- or Ca^{2+}-induced rigidization of the membrane appears to plateau at 150 μM or 2.2 mM. Since La^{3+} markedly inhibits $^{45}Ca^{2+}$ binding to low-affinity sites on isolated rat cardiac sarcolemma [71], La^{3+} and Ca^{2+} may each mediate

alterations in the lipid fluidity by binding to the same low-affinity sites. However, additional studies must be performed to determine whether the Ca^{2+} and La^{3+} fluidity effects are competitive.

Ca^{2+}-Sarcolemmal Binding Sites That Modulate the Membrane Fluidity: Possible Roles in Regulating Heart Function

Ca^{2+} plays central roles in the normal sequence of excitation and contraction in the beating heart. The cellular uptake of Ca^{2+} occurs during the plateau phase of the cardiac action potential, and extracellular Ca^{2+} is essential for the development of contractile force [74, 75]. Recent investigations have suggested that the inotropic state of the heart may be closely related to the amount of Ca^{2+} bound to low-affinity plasma membrane sites. The Ca^{2+} concentration at which half maximal binding to low-affinity sites on guinea pig cardiac sarcolemma occurs (ie, 0.5 mM) is similar to that which induces half-maximal increases in myocardial contractility [74]. It is therefore of interest that Ca^{2+} binding to low-affinity sites decreases the fluidity of rat heart plasma membranes. If Ca^{2+} displaced from low-affinity sites on the heart cell surface is the immediate source of contractile-dependent Ca^{2+}, as has been proposed by several authors [71, 75, 76], then both the Ca^{2+} levels bound to these sites and the membrane fluidity might demonstrate periodic fluctuations in the beating heart.

The above discussion suggests that the cyclical occupancy of Ca^{2+} sarcolemmal binding sites, and associated alterations in the membrane fluidity, may be involved in the excitation–contraction coupling process. The surface membrane of cardiac cells provides a selective permeability barrier to various substrates, interacts with certain hormones and ions that modulate heart activities, and undergoes ionic conductance changes involved in excitation–contraction coupling. As discussed earlier, each of these membrane functional processes may be sensitive to changes in the lipid fluidity. Thus, an intriguing possibility is that periodic Ca^{2+}-induced alterations in the sarcolemmal fluidity may provide an effective control of the metabolism and contractile behavior of the myocardium by regulating these membrane activities. Ca^{2+}, at concentrations that decrease the fluidity of I(12,3)-labeled rat heart plasma membrane, has indeed been found to alter many of those sarcolemmal functions that are sensitive to temperature-induced changes in the lipid structure. For example, mM Ca^{2+} inhibits the activities of Na^+, K^+-ATPase preparations from guinea pig hearts [77] and basal and epinephrine-stimulated AC of guinea pig heart plasma membranes [78]. Furthermore, 1 mM Ca^{2+} inhibits veratridine-stimulated uptake of Na^+ and Ca^{2+} in chick heart cells [62]. If the degree to which these processes are inhibited by Ca^{2+} is related to the occupancy of low-affinity membrane sites, then one mechanism by which Ca^{2+} regulates these activities may be by mediating fluctuations in the sarcolemmal fluidity.

An additional question that should be addressed is whether La^{3+}-induced alterations in the sarcolemmal fluidity are involved with the effects this cation exerts on various myocardial functions. Perfusion of intact hearts with μM La^{3+} rapidly uncouples excitation from contraction and also completely blocks mechanical activity [79]. Recent evidence indicates that these effects are due, in part, to the essentially irreversible displacement of contractile-dependent Ca^{2+} by La^{3+} and the subsequent inhibition of Ca^{2+} influx into the cell [75, 80]. In addition, La^{3+} (10–100 μM) increases the membrane resistance of guinea pig papillary muscle [81] and also inhibits the activities of Na^+, K^+-ATPase in guinea pig heart microsomes [73] and Ca^{2+}- and Mg^{2+}-ATPase in rat cardiac sarcolemma [82]. It is tempting, therefore, to speculate that alterations in the lipid fluidity induced by approximately 100 μM La^{3+} may regulate membrane electrical properties and/or ion fluxes

across the sarcolemma. In this context, Nayler and Harris reported that 10 to 100 μM La^{3+} has a dose-dependent, uncompetitive inhibitory effect of guinea pig heart microsomal Na^+,K^+-ATPase [73]; our spin-label studies on rat cardiac sarcolemma suggest that La^{3+} may indirectly inhibit Na^+,K^+-ATPase through decreases in the lipid fluidity which occur upon the binding of La^{3+} to constituent acidic phospholipids. Any alterations in the fluidity that accompany the cyclical occupancy of Ca^{2+} sarcolemmal binding sites would be expected to be blocked by La^{3+}, because of the strong association of La^{3+} to Ca^{2+}membrane sites.

Ca^{2+} Effects on Liver Plasma Membrane Fluidity and Associated Functions

Ca^{2+} may indirectly affect the activity of a variety of liver functions by altering the plasma membrane fluidity. As discussed earlier, the temperature dependence of various liver membrane enzymatic activities and transport processes indicated that these functions are influenced by the lipid structure. The observation that certain of these temperature-sensitive activities are also regulated by mM Ca^{2+} therefore suggests that Ca^{2+} additions and temperature alterations may modulate these processes through changes in the fluidities of lipid domains. For example, Na^+,K^+-ATPase and GSAC activities in liver plasma membrane are inhibited by mM Ca^{2+} [83, 84]. Furthermore, mM Ca^{2+} modulates the membrane permeability of Na^+ and K^+ ions in rat hepatocytes [85]. Although changes in the lipid fluidity may be one mechanism by which Ca^{2+} alters liver membrane activities, other regulating models involving direct cation–enzyme interactions cannot be excluded.

ACKNOWLEDGMENTS

The authors wish to thank Drs. Arne N. Wick, Urban J. Lewis, and Willard P. VanderLaan for the use of their facilities. Drs. Alfred Esser and Hans Müller-Eberhard graciously permitted us access to the ESR spectrometer. We also wish to acknowledge Dr. Miles Houslay for helpful discussions, and the reviewers for their comments on the presence of time constant averaging in the unexpanded spectra. This was supported by grants from the NIH (AM 21290-01 and HL-20517-02) and from the American Diabetes Association, Southern California Affiliate, Inc. L.M.G. was sponsored by a postdoctoral fellowship from the San Diego County Heart Association. This is Publication #14 from the Lutcher Brown Center for Diabetes and Endocrinology, Scripps Clinic and Research Foundation.

REFERENCES

1. Singer SJ, Nicolson GL: Science 175:720, 1972.
2. Martonosi MA: FEBS Lett 47:327, 1974.
3. Blazyk JF, Steim JM: Biochim Biophys Acta 266:737, 1972.
4. Jain MK, White HB: In Paoletti R, Kritchevsky D (eds): "Advances in Lipid Research." New York: Academic Press, 1977, p 1.
5. Lee AG, Birdsall NJM, Metcalfe JC, Toon PA, Warren GB: Biochemistry 13:3699, 1974.
6. Lee AG: Prog Biophys Mol Biol 29:3, 1975.
7. Phillips WC, Finer EG: Biochim Biophys Acta 356:199, 1974.
8. Papahadjopoulos D, Poste G: Biophys J 15:945, 1975.
9. Galla HJ, Sackmann E: Biochim Biophys Acta 401:509, 1975.
10. Ohnishi S, Ito T: Biochemistry 13:881, 1974.
11. Hartmann W, Galla HJ, Sackmann E: FEBS Lett 78:169, 1977.
12. Wu SH, McConnell HM: Biochemistry 14:847, 1975.

13. Esser A, Mack HM, Halverson CR, Souza KA: Fed Proc 37:1393, 1978.
14. McConnell HM: In Berliner LJ (ed): "Spin Labeling." New York: Academic Press, 1976, pp 525–560.
15. Hubbell WL, McConnell HM: J Am Chem Soc 93:314, 1971.
16. Butler K, Tattrie N, Smith ICP: Biochim Biophys Acta 363:351, 1974.
17. Oldfield E, Chapman D: FEBS Lett 23:285, 1972.
18. Oldfield E, Keough K, Chapman D: FEBS Lett 20:344, 1971.
19. Sauerheber RD, Gordon LM, Crosland RD, Kuwahara MD: J Memb Biol 31:131, 1977.
20. Evans WH: Biochem J 116:833, 1970.
21. Sauerheber RD, Gordon LM: Proc Soc Exp Biol Med 150:28, 1975.
22. Kidwai AM, Radcliffe M, Duchon G, Daniel E: Biochem Biophys Res Commun 45:901, 1971.
23. Sauerheber RD, Gordon LM, Esgate JA: manuscript in preparation.
24. Gaffney BJ, Methods Enzymol 32:161, 1974.
25. Ehrström M, Eriksson L, Israelachvili J, Ehrenberg A: Biochem Biophys Res Commun 55:396, 1973.
26. Gordon LM, Sauerheber RD: Biochim Biophys Acta 466:34, 1977.
27. Seelig J: J Am Chem Soc 29:3881, 1970.
28. Israelachvili J, Sjösten J, Eriksson L, Ehrström M, Gräslund A, Ehrenberg A: Biochim Biophys Acta 339:164, 1974.
29. Griffith OH, Jost PC: In Berliner LJ (ed): "Spin Labeling – Theory and Applications." New York: Academic Press, 1976, p 453.
30. Butterfield D, Roses A, Cooper M, Appel SH, Chesnut DB: Biochemistry 13:5078, 1974.
31. Sackmann E, Träuble H, Galla H, Overath P: Biochemistry 12:5360, 1973.
32. Nikaido H, Takeuchi Y, Ohnishi S, Nakae T: Biochim Biophys Acta 465:152, 1977.
33. Butterfield DA, Whisnant CC, Chesnut DB: Biochim Biophys Acta 426:697, 1976.
34. Verma S, Wallach D: Biochim Biophys Acta 382:73, 1975.
35. Devaux P, Scandella C, McConnell HM: J Magn Reson 9:474, 1973.
36. Sackmann E, Träuble H: J Am Chem Soc 94:4482, 1972.
37. Scandella CJ, Devaux P, McConnell HM: Proc Natl Acad Sci USA 69:2056, 1972.
38. Cannon B, Polnaszek C, Butler K, Eriksson L, Smith ICP: Arch Biochem Biophys 167:505, 1975.
39. Ohnishi S, Ito T: Biochem Biophys Res Commun 51:132, 1973.
40. Snipes W, Keith AD: Res Dev 21:22, 1970.
41. Chapman D: Q Rev Biophys 8:185, 1975.
42. Grisham CM, Barnett RE: Biochemistry 12:2635, 1974.
43. Keith AD, Sharnoff M, Cohn G: Biochim Biophys Acta 300:379, 1973.
44. Träuble H, Sackmann E: J Amer Chem Soc 94:4499, 1972.
45. Houslay MD, Hesketh TR, Smith GA, Warren GB, Metcalfe JC: Biochim Biophys Acta 436:495, 1976.
46. Jain MK, Wu NM: J Memb Biol 34:157, 1977.
47. Dipple I, Houslay MD: Biochem J (In press).
48. Hui SW, Parsons DF: Cancer Res 36:1918, 1976.
49. Bashford CL, Morgan CG, Radda GK: Biochim Biophys Acta 426:157, 1976.
50. Ting P, Solomon AK: Biochim Biophys Acta 406:447, 1975.
51. Lee AG: FEBS Lett 62:359, 1976.
52. Hui SW, Parsons DF: Science 190:383, 1975.
53. Feldman DA, Weinhold PA: Biochem Pharm 26:2283, 1977.
54. Jain MK: In Bronner, Kleinzeller (eds): "Current Topics in Membranes and Transport," vol. 6. New York: Academic Press, 1975, p 1.
55. Terris S, Steiner DF: J Biol Chem 250:8389, 1975.
56. Baur H, Heldt HW: Fur J Biochem 74:397, 1977.
57. Houslay MD, Johannsson A, Smith GA, Hesketh TR, Warren GB, Metcalfe JC: In Abrahamsson S, Pascher I (eds): "Structure of Biological Membranes," New York: Plenum Press, Nobel Foundation Symposium 34, 1976, p 331.
58. Keirns JJ, Kreiner PW, Bitensky MW: J Supramol Struc 1:368, 1973.
59. Riordan JR, Slavik M, Kertner N: J Biol Chem 252:5449, 1977.
60. Cuatrecasas P: Ann Rev Biochem 43:169, 1974.
61. Papahadjopoulos D, Jacobson K, Nirs S, Isac T: Biochim Biophys Acta 311:330, 1973.
62. Fossett M, De Barry J, Lenoir M, Lazdunski M: J Biol Chem 252:6112, 1977.
63. McMurchie E, Raison J, Cairncross K: Comp Biochem Physiol 44B:1017, 1973.
64. Coraboeuf E, Weidmann S: Helv Physiol Acta 12:32, 1954.

65. Mattiazzi AR, Nilsson E: Acta Physiol Scand 97:310, 1976.
66. Benfey BG: Fed Proc 36:2575, 1977.
67. Fourcans B, Jain MK: Adv Lipid Res 12:147, 1974.
68. Klein I, Moore L, Pastan I: Biochim Biophys Acta 506:42, 1978.
69. Sinha AK, Shattil SJ, Colman RW: J Biol Chem 252:3310, 1977.
70. Brivio-Haugland RP, Louis SL, Mucsh K, Waldeck N, Williams MA: Biochim Biophys Acta 433:150, 1976.
71. Limas CJ: Arch Biochem Biophys 179:302, 1977.
72. Shlatz L, Marinetti GV: Biochim Biophys Acta 290:70, 1972.
73. Nayler WG, Harris JP: J Mol Cell Card 8:811, 1976.
74. Williamson JR, Woodrow ML, Scarpa A: In Fleckenstein A, Dhalla NS (eds): "Recent Advances in Studies on Cardiac Structure and Metabolism," vol. 5. Baltimore: University Park Press, 1975, p 61.
75. Langer GA: Fed Proc 35:1274, 1976.
76. Lüllmann H, Peters T: Clin Exp Pharm Phys 4:49, 1977.
77. Godfraind T, De Pover A, Verbeke N: Biochim Biophys Acta 481:202, 1977.
78. Tada M, Kirchberger MA, Katz AM: In Roy P, Dhalla NS (eds): "Recent Advances in Studies on Cardiac Structure and Metabolism," vol. 9. Baltimore: University Park Press, 1976, p 117.
79. Williamson JR, Schaffer SW, Scarpa A, Safer B: In Roy P, Dhalla NS (eds): "Recent Advances in Studies on Cardiac Structure and Metabolism," vol. 3. Baltimore: University Park Press, 1974, p 375.
80. Langer GA, Frank JS: J Cell Biol 54:441, 1972.
81. Haass A: N-S Arch Pharmacol 290:207, 1975.
82. Anand MB, Chauhan MS, Dhalla NS: J Biochem 82:1731, 1977.
83. Boyer J, Reno D: Biochim Biophys Acta 401:59, 1975.
84. Hepp KD, Edel R, Wieland O: Eur J Biochem 17:171, 1970.
85. Kolb HA, Adam G: J Memb Biol 26:121, 1976.